

Transferrable Feature and Projection Learning with Class Hierarchy for Zero-Shot Learning

Aoxue Li · Zhiwu Lu · Jiechao Guan · Tao Xiang · Liwei Wang · Ji-Rong Wen

Received: date / Accepted: date

Abstract Zero-shot learning (ZSL) aims to transfer knowledge from seen classes to unseen ones so that the latter can be recognised without any training samples. This is made possible by learning a projection function between a feature space and a semantic space (e.g. attribute space). Considering the seen and unseen classes as two domains, a big domain gap often exists which challenges ZSL. Inspired by the fact that an unseen class is not exactly ‘unseen’ if it belongs to the same superclass as a seen class, we propose a novel inductive ZSL model that leverages superclasses as the bridge between seen and unseen classes to narrow the domain gap. Specifically, we first build a class hierarchy of multiple superclass layers and a single class layer, where the superclasses are automatically generated by data-driven clustering over the semantic representations of all seen and unseen class names. We then exploit the superclasses from the class hierarchy to tackle the domain gap challenge in two aspects: deep feature learning and projection function learning. First, to narrow the domain gap in the feature space, we integrate a recurrent neural network (RNN) defined with the superclasses into a convolutional neural network (CNN), in order to enforce the superclass hierarchy. Second, to

further learn a transferrable projection function for ZSL, a novel projection function learning method is proposed by exploiting the superclasses to align the two domains. Importantly, our transferrable feature and projection learning methods can be easily extended to a closely related task – few-shot learning (FSL). Extensive experiments show that the proposed model significantly outperforms the state-of-the-art alternatives in both ZSL and FSL tasks.

Keywords Zero-shot learning · Class hierarchy · Recurrent neural network · Deep feature learning · Projection function learning · Few-shot learning

1 Introduction

In the past five years, deep neural network (DNN) based models (Huang et al., 2017; Donahue et al., 2014) have achieved super-human performance on the ILSVRC 1K recognition task. However, most existing object recognition models, particularly those DNN-based ones, require hundreds of image samples to be collected for each object class; many of the object classes are rare and it is thus extremely hard, sometimes impossible to collect sufficient training samples, even with social media. One way to bypass the difficulty in collecting sufficient training data for object recognition is zero-shot learning (ZSL) (Rahman et al., 2017; Li et al., 2017a; Zhang and Saligrama, 2016b; Chao et al., 2016). The goal of ZSL is to recognise a new/unseen class without any training samples from the class. A ZSL model typically assumes that each class name is embedded in a semantic space. With this semantic space and a visual feature space representing the appearance of an object in an image, it chooses a joint embedding space (which is mostly formed with the semantic space) and learns a projection function so that both the visual features and the semantic vectors are embedded in the same space. Under the inductive

A. Li and L. Wang

The Key Laboratory of Machine Perception (MOE), School of Electronics Engineering and Computer Science, Peking University, Beijing 100871, China

E-mail: lax@pku.edu.cn

Z. Lu, J. Guan and J. Wen

The Beijing Key Laboratory of Big Data Management and Analysis Methods, School of Information, Renmin University of China, Beijing 100872, China

E-mail: zhiwu.lu@gmail.com

T. Xiang

The School of Electronic Engineering and Computer Science, Queen Mary University of London, Mile End Road, London E1 4NS, United Kingdom

E-mail: t.xiang@qmul.ac.uk.

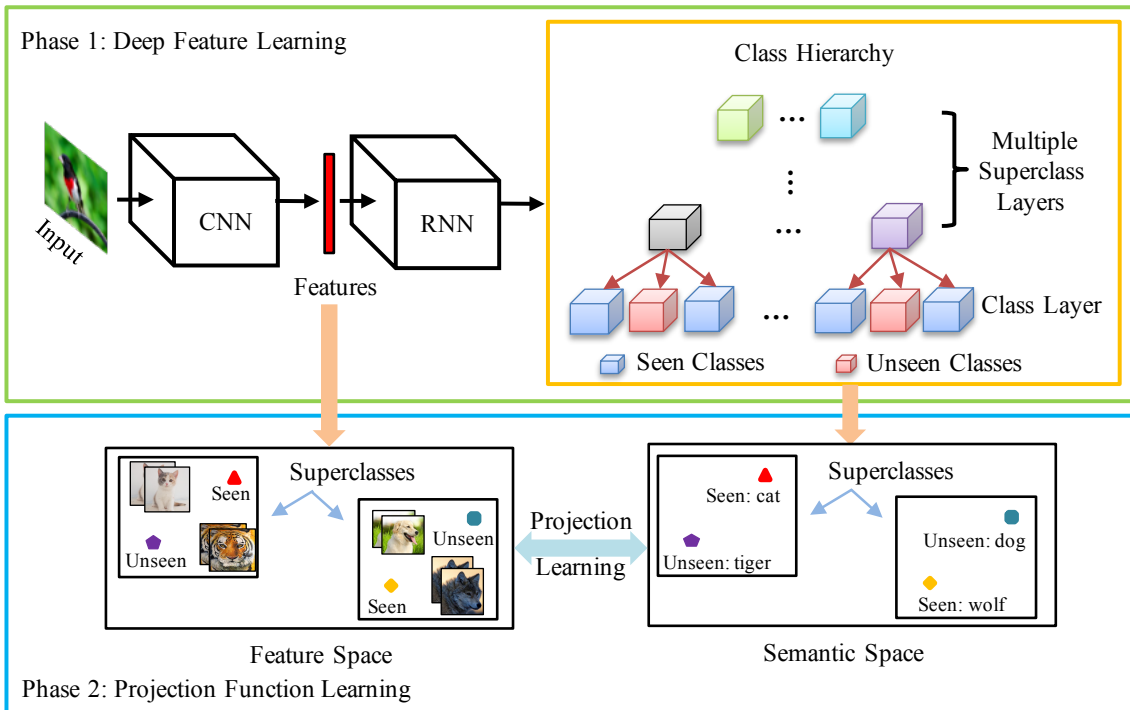


Fig. 1 Overview of the proposed model for inductive ZSL with class hierarchy (including deep feature learning and projection function learning).

ZSL setting, the projection function is learned only with the seen class training samples and then directly used to project the unseen class samples to the joint embedding space. The class label of a test unseen class sample is assigned to the nearest unseen class prototype.

One of the biggest challenges in ZSL is the domain gap between the seen and unseen classes. As mentioned above, the projection functions learned from the seen classes are applied to the unseen class data. However, the unseen classes are often visually very different from the seen ones; therefore the domain gap between the seen and unseen class domains can be big, meaning that the same projection function may not be able to project an unseen class image to be close to its corresponding class name in the joint embedding space for correct recognition.

To tackle the domain gap challenge, most previous works focus on learning more transferrable projection functions. Specifically, many ZSL models resort to transductive learning (Ye and Guo, 2017; Guo et al., 2016; Kodirov et al., 2015), where the unlabeled test samples from unseen classes are used to learn the projection functions. However, such an approach assumes the access to the whole test dataset beforehand, and thus deviates from the motivation of ZSL: the unseen class samples are rare. These transductive ZSL models are thus limited in their practicality in real-world scenarios. Moreover, other than projection function learning, deep feature learning has been largely overlooked in ZSL. Most previous works, if not all, simply use visual

features extracted by convolutional neural network (CNN) models pretrained on ImageNet (Russakovsky et al., 2015). We argue that deep feature learning and projection function learning should be equally important for overcoming the domain gap challenge.

In this paper, we propose a novel inductive ZSL model that leverages the superclasses as the bridge between seen and unseen classes to narrow the domain gap. The idea is simple: an unseen class is not strictly ‘zero-shot’ if it falls into a superclass that contains one or more seen classes. Exploiting the shared superclass among seen and unseen classes thus provides a means for narrowing the domain gap. In this work, we generate the superclasses by a data-driven approach, without the need of a human-annotated taxonomy. Specifically, we construct a tree-structured class hierarchy that consists of multiple superclass layers and a single class layer. In this tree-structured hierarchy, we take both seen classes and unseen classes as the leaves, and generate the superclasses by clustering over the semantic representations of all seen and unseen class names (see the orange box in Fig. 1). Moreover, by exploiting the superclasses from the class hierarchy, the proposed model aims to narrow the domain gap in two aspects: deep feature learning and projection function learning.

To learn transferrable visual features, we propose a novel deep feature learning model based on the superclasses from the class hierarchy. Specifically, a CNN model is first designed for both class and superclass classification.

Since the seen and unseen classes may have the same superclasses, directly training this CNN model enables us to learn transferrable deep features. To further strengthen the feature transferability, we explicitly encode the hierarchical structure among classes/superclasses into the CNN model, by plugging recurrent neural network (RNN) (Graves et al., 2013; Zheng et al., 2015; Liu et al., 2017) components into the network. Overall, a novel CNN-RNN architecture is designed for transferrable deep feature learning, as illustrated in the green box in Fig. 1.

To learn a transferrable projection function for inductive ZSL, we propose a novel projection function learning method by utilising the superclasses to align the two domains, as shown in the blue box in Fig. 1. Specifically, we formulate the projection function learning on each superclass layer as a graph regularised self-reconstruction problem. An efficient iterative algorithm is developed as the solver. The results of multiple superclass layers are combined to boost the performance of projection function learning on the single class layer.

Importantly, our model can be easily extended to a closely related problem – few-shot learning (FSL) (Snell and Zemel, 2017; Qiao et al., 2018; Finn et al., 2017; Sung et al., 2018). Specifically, the above transferrable feature and projection learning methods involved in our model are employed to solve the FSL problem without any modification. Experiments on the widely-used mini-ImageNet dataset (Snell and Zemel, 2017) show that our model achieves the state-of-the-art results. This suggests that the class hierarchy is also important for narrowing down the domain gap in the FSL problem.

Our contributions are: (1) A novel inductive ZSL model is proposed to align the seen and unseen class domains by utilising the superclasses shared across the two domains. To our best knowledge, this is the first time that the superclasses generated by data-driven clustering have been leveraged in both feature learning and projection learning to narrow the domain gap for inductive ZSL. (2) Due to the domain alignment using the superclasses from the class hierarchy, we have created the new state-of-the-art for ZSL and FSL.

2 Related Work

2.1 Semantic Space

Three semantic spaces are typically used for ZSL: the attribute space (Zhang and Saligrama, 2015; Guo et al., 2016; Shojaaee and Baghshah, 2016), the word vector space (Frome et al., 2013; Norouzi et al., 2014; Fu et al., 2015b), and the textual description space (Reed et al., 2016; Alexiou et al., 2016; Fu and Sigal, 2016). The attribute space is the most widely-used semantic space. However, for large-scale problems, annotating attributes for each class becomes

very difficult. Recently, the semantic word vector space has begun to be popular especially in large-scale problems (Fu et al., 2015b; Kodirov et al., 2015), since no manually defined ontology is required and any class name can be represented as a word vector for free. Beyond semantic attribute or word vector, the semantic space can also be created by directly learning from textual descriptions of categories such as Wikipedia articles (Fu and Sigal, 2016) and sentence descriptions (Reed et al., 2016).

2.2 Projection Domain Shift

To overcome the projection domain shift (Fu et al., 2015a) caused by the domain gap in ZSL, transductive ZSL has been proposed to learn the projection function with not only labelled data from seen classes but also unlabelled data from unseen classes. According to whether the predicted labels of the test images are iteratively used for model learning, existing transductive ZSL models can be divided into two groups: (1) The first group of models (Fu et al., 2015a,b; Rohrbach et al., 2013; Ye and Guo, 2017) first constructs a graph in the semantic space and then the domain gap is reduced by label propagation (Wang and Zhang, 2008) on the graph. A variant is the structured prediction model (Zhang and Saligrama, 2016b) which utilises a Gaussian parameterisation of the unseen class domain label predictions. (2) The second category of models (Guo et al., 2016; Kodirov et al., 2015; Li et al., 2015; Shojaaee and Baghshah, 2016; Wang and Chen, 2017; Yu et al., 2017) involve using the predicted labels of the unseen class data in an iterative model update/adaptation process as in self-training (Xu et al., 2015, 2017). However, these transductive ZSL models assume the access to the whole test dataset, which is often invalid in the context of ZSL because new classes typically appear dynamically and unavailable before model learning. Instead of assuming the access to all test unseen class data for transductive learning, our model is developed based on inductive learning, and it resorts to learning visual features and projection function only with the training labelled seen class data to counter the projection domain shift.

2.3 ZSL with Superclasses

In the area of ZSL, little attention has been paid to ZSL with superclasses. There are only two exceptions. One is (Hwang and Sigal, 2014), which learns the relation between attributes and superclasses for semantic embedding, and the other is (Akata et al., 2015) which utilises superclasses to define a semantic space for ZSL. However, the superclasses used in these works are obtained from the manually-defined hierarchical taxonomy, which needs additional cost to collect. In this paper, our model is more flexible by generating

superclasses automatically with data-driven clustering over semantic representations of all seen/unseen class names. In addition, the superclasses are not induced into the feature learning in (Akata et al., 2015; Hwang and Sigal, 2014).

2.4 ZSL with Feature Learning

Most existing ZSL models extract visual features by using CNNs pretrained on ImageNet. This is to assume that the feature extraction model will generalise equally well for seen and unseen classes. This assumption is clearly invalid, particularly under the recently proposed ‘pure’ ZSL setting (Xian et al., 2017), where the unseen classes have no overlapping with the ImageNet 1K classes used to train the feature extraction model. The only notable exception is (Long et al., 2017) which uses the central loss and fine-tunes ImageNet pretrained deep model on seen classes. However, without any transferrable learning module, the feature extraction model proposed in (Long et al., 2017) has no guarantee of generalising well to unseen classes.

2.5 Label Correlation Modeling

Although no existing ZSL work has considered modeling label correlations to address the domain gap issue, the idea of using the relationship of class labels to improve multi-label classification has been exploited (Deng et al., 2014; Zheng et al., 2015; Liu et al., 2017). The label relationship has been modeled as hierarchy and exclusion graph (HEX) (Deng et al., 2014), CRF (Zheng et al., 2015) or RNN (Liu et al., 2017). Our model differs in two aspects: (1) It is designed to learn transferrable deep features and projection functions, rather than making more accurate label prediction; and (2) the label correlation is guided by a class hierarchy rather than exhaustive as in CRF (Zheng et al., 2015) and defined by the label frequency as in RNN (Liu et al., 2017).

2.6 Few-Shot Learning

Few-shot learning (FSL) (Snell and Zemel, 2017; Qiao et al., 2018; Finn et al., 2017; Sung et al., 2018) aims to recognise novel classes from very few labelled examples. Such label scarcity issue challenges the standard fine-tuning strategy used in deep learning. Data augmentation can alleviate the label scarcity issue, but cannot solve it. The latest FSL approaches thus choose to transform the deep network training process to meta learning where the transferrable knowledge is learned in the form of good initial conditions, embeddings, or optimisation strategies (Finn et al., 2017; Sung et al., 2018). In this paper, we directly employ our transferrable feature learning and projection learning methods to solve FSL task. Experimental results in Sec. 4.2

demonstrate that, similar to the ZSL task, our transferrable feature learning and projection learning methods can also achieve state-of-the-art results in the FSL task.

3 Methodology

3.1 Problem Definition

We first formally define the ZSL problem as follows. Let $S = \{s_1, \dots, s_p\}$ denote the set of seen classes and $U = \{u_1, \dots, u_q\}$ denote the set of unseen classes, where p and q are the total numbers of seen classes and unseen classes, respectively. These two sets of classes are disjoint, i.e. $S \cap U = \phi$. We are given a set of labelled training images $D_s = \{(I_i, y_i, f_i, z_i) : i = 1, \dots, N_s\}$, where I_i denotes the i -th image in the training set, $y_i \in S$ denotes its corresponding label, f_i denotes its d_f dimensional visual feature vector, z_i denotes its d_z dimensional semantic representation of the corresponding class, and N_s denotes the total number of labelled images. Let $D_u = \{(I_j, y_j, f_j, z_j) : j = 1, \dots, N_u\}$ denote a set of unlabelled test images, where I_j denotes the j -th image in the test set, $y_j \in U$ denotes its corresponding unknown labels, f_j denotes its d_f dimensional visual feature vector, z_j denotes its d_z dimensional semantic representation of the corresponding class, and N_u denotes the total number of unlabelled images. We thus have the training seen class feature matrix $F_s = [f_i]_{N_s \times d_f}$, the test unseen class feature matrix $F_u = [f_j]_{N_u \times d_f}$, and the training seen class semantic matrix $Z_s = [z_i]_{N_s \times d_z}$. The goal of inductive ZSL is to predict the unseen class sample labels $\{y_j : j = 1, \dots, N_u\}$ using a model trained with the seen class data D_s only. In a generalised ZSL setting, the test samples come from both seen and unseen classes, and the ZSL problem becomes more realistic yet more challenging.

Our approach to inductive ZSL consists of three main components: class hierarchy construction, deep feature learning with superclasses, and projection function learning with superclasses. Their details are given below.

3.2 Class Hierarchy Construction

In this section, we describe how to construct a tree-structured class hierarchy using a data-driven approach. The class hierarchy consists of multiple superclass layers and one single class layer. Starting from the bottom class nodes (i.e. both seen and unseen classes), we obtain the nodes in the upper layer by clustering the nodes in the lower layer, forming a tree-structured class hierarchy (see the red dashed box in Fig. 2). We thus obtain a set $R = \{r_l : l = 1, \dots, n_r\}$ that collects the number of clusters at each superclass layer, where r_l denotes the number of clusters in the l -th superclass layer, and n_r denotes the total number of superclass layers

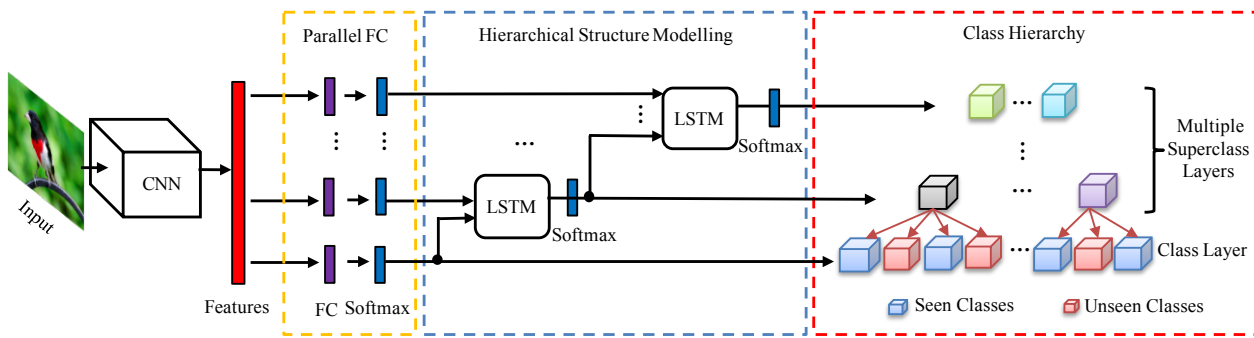


Fig. 2 Overview of the proposed CNN-RNN model for deep feature learning with three-layer class hierarchy.

in the class hierarchy. Each class label y_i can be mapped to its corresponding superclasses $V_i = \{v_i^l : l = 1, \dots, n_r\}$, where v_i^l denotes the superclass label of y_i in the l -th superclass layer. This results in multiple labels at different class/superclass levels for the image I_i . More concretely, at each layer of the tree-structured hierarchy, we cluster the nodes by their semantic representations. Each cluster then forms a parent node (i.e. a superclass) in the upper layer of the tree. In this way, the semantic representation of the superclass is, in a sense, a mixing of the semantics of its children classes. Since the superclass labels are shared across both seen and unseen class domains, the proposed model can overcome the domain gap challenge for ZSL.

3.3 Deep Feature Learning

In this section, we describe our feature extraction model, which is learned only using the seen class data D_s (along with the class hierarchy constructed using semantic representations of all seen and unseen names) but expected to represent well the unseen class data D_u . In this paper, we propose a CNN-RNN model defined with superclasses from the aforementioned class hierarchy to learn transferrable visual features for unseen class samples. This deep feature learning model takes an image I_i as the input and then outputs a d_f -dimensional feature vector $f_i = \phi(I_i) \in \mathbb{R}^{d_f}$. Concretely, we extend a CNN model by two steps for predicting the superclass-level labels, using the shared CNN generated features f_i . The first step is to predict the labels at different class/superclass levels (see the yellow dashed box in Fig. 2), so that the shared superclasses at those layers can make the learned features suitable for representing the unseen classes. The second step is to encode the hierarchical structure of class/superclass layers into superclass label prediction. That is, we infer each superclass label by considering the prediction results of the same or lower class/superclass layers (see the blue dashed box in Fig. 2). We are essentially learning a hierarchical classifier – the features learned need to be useful for not only recognising the leaf-level classes, but

also the higher level classes/superclasses, which are shared with the unseen classes. This makes sure that the learned feature are relevant to the unseen classes, even without using any samples from those classes. In this work, we propose to exploit the hierarchical structure using an RNN model. When RNN is combined with CNN, we obtain a CNN-RNN model for deep feature learning. We will give its technical details in the following.

For the first class/superclass label prediction step, we add $n_r + 1$ parallel fully-connected (FC) layers along with softmax layers on top of the CNN model for feature extraction, as shown in the yellow dashed box in Fig. 2. Given an object sample, each fully-connected layer with softmax thus predicts the probability distribution of the corresponding-level classes (i.e. class/superclass-level). We further introduce an RNN to model the hierarchical structure between layers and integrate this label-relation encoding module with the label prediction steps. More specifically, we model the hierarchical structure among multiple class/superclass layers by n_r Long-Short-Term-Memory (LSTM) networks.

Formally, an LSTM unit has two types of states: cell state c and hidden state h . As in (Graves et al., 2013), a forward pass at time t with input x_t is computed as follows:

$$\begin{aligned}
 i_t &= \sigma(W_{i,h} \cdot h_{t-1} + W_{i,c} \cdot c_{t-1} + W_{i,x} \cdot x_{t-1} + b_i) \\
 f_t &= \sigma(W_{f,h} \cdot h_{t-1} + W_{f,c} \cdot c_{t-1} + W_{f,x} \cdot x_{t-1} + b_f) \\
 o_t &= \sigma(W_{o,h} \cdot h_{t-1} + W_{o,c} \cdot c_{t-1} + W_{o,x} \cdot x_{t-1} + b_o) \\
 g_t &= \tanh(W_{g,h} \cdot h_{t-1} + W_{g,c} \cdot c_{t-1} + W_{g,x} \cdot x_{t-1} + b_g) \\
 c_t &= f_t * c_{t-1} + i_t * g_t \\
 h_t &= o_t * \tanh(c_t)
 \end{aligned} \tag{1}$$

where c_t and h_t are the models' cell and hidden states, i_t , f_t , o_t are respectively the activations of input gate, forget gate, and output gate, $W_{\cdot,h}$, $W_{\cdot,c}$ are the recurrent weights, $W_{\cdot,x}$ are the input weights, and b_{\cdot} are the biases. Here, $\sigma(\cdot)$ is defined with the sigmoid function.

In this paper, to model the hierarchical structure among class/superclass-level labels in the first two layers (from bottom), we use an LSTM network with two time steps. In the first time step, the output of class-level fully-connected

layer (with softmax) is used as input; and in the next time step, the output of superclass-level fully-connected layer (with softmax) is used as input and the hidden cell predicts the probability distribution of superclass-level labels. The formal formulation of this LSTM network is given as:

$$\begin{aligned} [h'_1, c'_1] &= \text{LSTM}(p_0, h_0, c_0) \\ [h_1, c_1] &= \text{LSTM}(p_1, h'_1, c'_1) \\ \hat{p}_1 &= \text{softmax}(\hat{W}_1 \cdot h_1 + \hat{b}_1) \end{aligned} \quad (2)$$

where p_0 denotes the output of fully-connected layer corresponding to class-level. p_1 denotes the output of fully-connected layer corresponding to superclass-level. h_0 (or h'_1, h_1) and c_0 (or c'_1, c_1) are the initial (or intermediate) hidden state and cell state. $\text{LSTM}(\cdot)$ is a forward step of an LSTM unit. \hat{W}_1 and \hat{b}_1 are the weight and bias of the output layer, respectively. The output \hat{p}_1 defines a distribution over possible superclass-level labels.

Moreover, to model the hierarchical structure among classes/superclasses in the first l ($l \geq 3$) layers, we also employ a two-time-step LSTM network. Concretely, in the first time step, we feed the output of the previous LSTM as input, since the previous LSTM has fused all information of the first $l - 1$ layers. In the next time step, the output of the current superclass-level fully-connected layer (with softmax) is used as input and the hidden cell predicts the probability distribution of the current superclass-level labels (see the blue dashed box in Fig. 2). We thus provide the formal formulation of the LSTM network as follows:

$$\begin{aligned} [h'_{l-1}, c'_{l-1}] &= \text{LSTM}(\hat{p}_{l-1}, h_{l-1}, c_{l-1}) \\ [h_l, c_l] &= \text{LSTM}(p_l, h'_{l-1}, c'_{l-1}) \\ \hat{p}_l &= \text{softmax}(\hat{W}_l \cdot h_l + \hat{b}_l) \end{aligned} \quad (3)$$

where \hat{p}_{l-1} denotes the output of the previous LSTM. p_l denotes the output of the l -th fully-connected layer. h_{l-1} and c_{l-1} are the hidden state and cell state of the previous LSTM network. h'_{l-1} (or h_l) and c'_{l-1} (or c_l) are the intermediate hidden state and cell state of the current LSTM network. \hat{W}_l and \hat{b}_l are the corresponding weight and bias of the output layer. The output \hat{p}_l defines a distribution over possible superclass-level labels in the l layer of the class hierarchy. With this method, we can obtain a total of n_r two-time-step LSTM networks to model the hierarchical structure among the superclasses/classes in the hierarchy.

Therefore, by merging the hierarchical structure modelling with the original class label prediction, we define the loss function for an image x as follows:

$$\begin{aligned} \mathcal{L}(\theta_F, \theta_c, \theta_s) &= \mathcal{L}_c(y, G_c(G(x; \theta_F); \theta_c)) \\ &+ \sum_{l=1}^{n_r} \lambda_l \mathcal{L}_{s_l}(v_l, G_{s_l}(G(x; \theta_F); \theta_{s_l})) \end{aligned} \quad (4)$$

where $\mathcal{L}_{s_l}(G_{s_l}, \theta_{s_l})$ denotes the loss (network, parameters) of the l -th LSTM which models the hierarchical structure among classes/superclasses in the first $l + 1$ layer. y and $\{v_l : l = 1, \dots, n_r\}$ denote the true label of the image at class level and n_r superclass levels, respectively. θ_F (or G) denotes the parameters (or network) of the CNN. $\mathcal{L}_c(G_c, \theta_c)$ denotes the loss (network, parameters) of class-level label prediction. λ_l weights these losses.

3.4 Projection Function Learning

Once the feature extraction model is learned using the training seen class data, it can be used to extract visual features from both training and test images and then compute the two feature matrices F_s and F_u for the seen and unseen class domains, respectively. With the seen class feature matrix F_s , we propose a novel projection learning method which exploits the superclasses from the class hierarchy to align the seen and unseen class domains. Since the superclasses are shared across the two domains, the proposed method enables us to learn a transferrable projection function for inductive ZSL. We give the details of our method below.

3.4.1 Projection Learning over Superclasses

As mentioned in Sec. 3.2, each class label y_i can be mapped to its corresponding superclasses $V_i = \{v_i^l : l = 1, \dots, n_r\}$, where v_i^l denotes the superclass label of y_i in the l -th superclass layer of the class hierarchy. Let e_i^l denote the d_z dimensional semantic vector of the superclass label v_i^l . We thus obtain n_r training superclass semantic matrices $\{E_s^l = [e_i^l]_{N_s \times d_z}, l = 1, \dots, n_r\}$, where each matrix collects the semantic vectors of superclasses in the corresponding layer for all seen class samples.

Given the training seen class feature matrix $F_s \in \mathbb{R}^{N_s \times d_f}$ and the initial training superclass semantic matrix $E_s^l \in \mathbb{R}^{N_s \times d_z}$, we model the set of seen class images as a graph $\mathcal{G} = \{\mathcal{W}, V\}$ with its vertex set $V = F_s$ and weight matrix $\mathcal{W} = \{w_{uv}\}$, where w_{uv} denotes the similarity between visual features of the u -th and v -th seen class images (i.e. f_u and f_v). It should be noted that the weight matrix \mathcal{W} is usually assumed to be nonnegative and symmetric. We thus compute the normalised Laplacian matrix \mathcal{L} of the graph \mathcal{G} by the following equation:

$$\mathcal{L} = I - D^{-1/2} \mathcal{W} D^{-1/2} \quad (5)$$

where I is an $N_s \times N_s$ identity matrix, and D is an $N_s \times N_s$ diagonal matrix with its u -th diagonal entry $\sum_v w_{uv}$.

Based on the well-known Laplacian regularisation and superclass semantic representations, our projection learning method solves the following optimisation problem with

respect to the l -th superclass layer:

$$\begin{aligned} & \min_{W^l, \tilde{E}_s^l} L(W^l, \tilde{E}_s^l) \\ & = \|F_s W^l - \tilde{E}_s^l\|_F^2 + \mu^l \|F_s - \tilde{E}_s^l W^{lT}\|_F^2 \\ & \quad + \epsilon^l \text{tr}(\tilde{E}_s^{lT} \mathcal{L} \tilde{E}_s^l) + \nu^l \|\tilde{E}_s^l - E_s^l\|_F^2 + \eta^l \|W^l\|_F^2 \end{aligned} \quad (6)$$

where $W^l \in \mathbb{R}^{d_f \times d_z}$ is the projection matrix between the superclass semantic representation corresponding to the l -th superclass layer and the visual feature representation, and $\tilde{E}_s^l \in \mathbb{R}^{N_s \times d_z}$ is the updated training superclass semantic matrix during model learning.

In the above objective function, the first two terms aim to learn bidirectional linear projections between F_s and \tilde{E}_s^l , which in fact is a self-reconstruction task (Kodirov et al., 2017) and has been verified to have good generalisation ability. Moreover, the third term denotes the well-known graph regularisation, which can enforce the superclass semantic representations \tilde{E}_s^l to preserve the graph locality of image features F_s , which benefits the feature self-reconstruction. The fourth term is a fitting constraint between \tilde{E}_s^l and E_s^l , meaning the the instance-level semantic representations should be close to their superclass prototype. The last term is the Frobenius norm used to regularise W^l . These terms are weighed by the four regularisation parameters $\mu^l, \epsilon^l, \nu^l, \eta^l$.

We further develop an efficient approach to tackle the graph regularised self-reconstruction problem in Eq. (6). Specifically, we solve Eq. (6) by alternately optimising the following two subproblems:

$$W^{l*} = \arg \min_{W^l} L(W^l, \tilde{E}_s^{l*}) \quad (7)$$

$$\tilde{E}_s^{l*} = \arg \min_{\tilde{E}_s^l} L(W^{l*}, \tilde{E}_s^l) \quad (8)$$

Here, \tilde{E}_s^{l*} is initialised with E_s^l . Taking a convex quadratic formulation, each of the above two subproblems has a global optimal solution. The two solvers are given below.

For the first subproblem, with $\tilde{E}_s^l = \tilde{E}_s^{l*}$ fixed, the solution of $\arg \min_{W^l} L(W^l, \tilde{E}_s^{l*})$ can be found by setting $\frac{\partial L(W^l, \tilde{E}_s^{l*})}{\partial W^l} = 0$. We thus obtain a linear equation:

$$(F_s^T F_s + \eta^l I) W^l + \mu^l W^l (E_s^{l*})^T E_s^{l*} = (1 + \mu^l) F_s^T E_s^{l*} \quad (9)$$

Let $\alpha^l = \mu^l / (1 + \mu^l) \in (0, 1)$ and $\gamma^l = \eta^l / (1 + \mu^l)$. In this paper, we empirically set $\gamma^l = 0.01$. We have:

$$[(1 - \alpha^l) F_s^T F_s + \gamma^l I] W^l + W^l (\alpha^l (E_s^{l*})^T E_s^{l*}) = F_s^T E_s^{l*} \quad (10)$$

which can be viewed as a Sylvester equation. Since $(1 - \alpha^l) F_s^T F_s + \gamma^l I \in \mathbb{R}^{d_f \times d_f}$ and $\alpha^l (E_s^{l*})^T E_s^{l*} \in \mathbb{R}^{d_z \times d_z}$

Algorithm 1: Projection Learning over Superclasses

Input: Training seen class feature matrix F_s
Initial training superclass semantic matrix E_s^l
Parameters $\alpha^l, \beta^l, \epsilon^l$

Output: W^{l*}

1. Set $\tilde{E}_s^{l*} = E_s^l$;
2. Construct a graph \mathcal{G} and compute \mathcal{L} with Eq. (5);

repeat

3. Find the best solution W^{l*} by solving Eq. (10);

4. Updating \tilde{E}_s^l with W^{l*} by solving Eq. (12);

until a stopping criterion is met

($d_f, d_z \ll N_s$), this equation can be solved efficiently by the Bartels-Stewart algorithm (Bartels and Stewart, 1972).

For the second subproblem, with $W^l = W^{l*}$ fixed, the solution of $\arg \min_{\tilde{E}_s^l} L(W^{l*}, \tilde{E}_s^l)$ can be found by setting $\frac{\partial L(W^{l*}, \tilde{E}_s^l)}{\partial \tilde{E}_s^l} = 0$. We thus have:

$$\begin{aligned} & \tilde{E}_s^l (\mu^l (W^{l*})^T W^{l*} + (1 + \nu^l) I) + \epsilon^l \mathcal{L} \tilde{E}_s^l \\ & = (1 + \mu^l) F_s W^{l*} + \nu^l E_s^l \end{aligned} \quad (11)$$

Let $\beta^l = 1 / (1 + \nu^l) \in (0, 1)$. We obtain:

$$\begin{aligned} & \tilde{E}_s^l [\alpha^l \beta^l (W^{l*})^T W^{l*} + (1 - \alpha^l) I] + \epsilon^l \mathcal{L} \tilde{E}_s^l \\ & = \beta^l F_s W^{l*} + (1 - \alpha^l) (1 - \beta^l) E_s^l \end{aligned} \quad (12)$$

which is a Sylvester equation. Since $\alpha^l \beta^l (W^{l*})^T W^{l*} + (1 - \alpha^l) I \in \mathbb{R}^{d_z \times d_z}$ ($d_z \ll N_s$), this equation can be solved efficiently by the Bartels-Stewart algorithm. Importantly, the time complexity of solving Eqs. (10) and (12) is linear with respect to the number of samples. Given that the proposed algorithm is shown to converge very quickly, it is efficient even for large-scale problems.

To sum up, we outline the proposed projection function learning method in Algorithm 1. Once the best projection function is learned, we first project the superclass prototypes corresponding to the l -th superclass layer into the feature space. We then perform nearest neighbour search over the possible superclasses (obtained from the higher-level superclass layer as described in Sec. 3.4.2) in the feature space to predict the superclass labels corresponding to the l -th superclass layer for test samples.

Note that we do not directly exploit the CNN-RNN model proposed in Sec. 3.3 to predict the superclass labels of the test unseen class samples, because *this model would fail when some superclasses only contain unseen classes*¹. In contrast, our projection learning method addresses this issue by projecting the superclass semantic representations to the feature space and then performing nearest neighbor search over these superclass prototypes for label inference.

¹ Our CNN-RNN model can still extract transferrable features for these test unseen class samples because the corresponding unseen classes share higher-level superclasses with some seen classes.

Algorithm 2: Full ZSL Algorithm

Input: Training set of seen class images D_s
 Test set of unseen class images D_u
 Parameters $\lambda_l, \alpha^l, \beta^l, \epsilon^l, \alpha^c, \beta^c, \epsilon^c$

Output: Labels of test samples

Class Hierarchy Construction:

1. Construct the tree-structured class hierarchy as in Sec. 3.2;

Deep Feature Learning:

2. Train a CNN-RNN model according to Eq. (4);
 3. Compute feature matrices F_s for the seen class domain;

Projection Function Learning:

4. Solve Eq. (6) for predicting the superclass labels using Algorithm 1;
 5. Generate the set of the most possible unseen class labels for each test sample;
 6. Solve Eq. (13) with an algorithm similar to Algorithm 1;
 7. Predict the unseen class label of each test sample.

3.4.2 Full ZSL Algorithm

The results of the proposed projection learning method can be used for inferring the labels of unseen class samples as follows. First, with respect to the current layer of the class hierarchy, we predict the top 3 superclass labels of each test unlabelled unseen sample x_j using the optimal projection matrix learned by Algorithm 1. Second, derived from the top 3 superclass labels of x_j , we obtain the set of the most possible superclass labels of x_j according to the lower-level superclass layer of the class hierarchy. In the same way, the set of the most possible unseen class labels $\mathcal{N}(x_j)$ can be acquired for the single class/leaf layer. Finally, we learn the projection function using seen class samples to infer the labels of unseen class samples by solving:

$$\begin{aligned} & \min_{W, \tilde{Z}_s} L(W, \tilde{Z}_s) \\ & = \|F_s W - \tilde{Z}_s\|_F^2 + \mu^c \|F_s - \tilde{Z}_s W^T\|_F^2 \\ & + \epsilon^c \text{tr}(\tilde{Z}_s^T \mathcal{L} \tilde{Z}_s) + \nu^c \|\tilde{Z}_s - Z_s\|_F^2 + \eta^c \|W\|_F^2 \end{aligned} \quad (13)$$

where $W \in \mathbb{R}^{d_f \times d_z}$ is the projection matrix, and $\tilde{Z}_s \in \mathbb{R}^{N_s \times d_z}$ is the updated training seen class semantic matrix during model learning. To solve this optimisation problem, we can develop a solver similar to Algorithm 1 (also need to tune parameters α^c, β^c and ϵ^c as Algorithm 1) and the only difference is that the training superclass semantic matrix is replaced by the class-level semantic matrix. When the best projection matrix is learned, we can project the class-level semantic prototypes from the test set into the feature space. The nearest neighbor search is then performed (over the set of the most possible unseen class labels) in the feature space to predict the label of a test image.

Different from existing projection learning methods that mainly rely on class-level semantics for label inference, we exploit both class-level and superclass-level semantics to recognise unseen class samples. Since the superclasses in

Table 1 Details of four benchmark datasets. Notations: ‘SS’ – semantic space, ‘SS-D’ – the dimension of semantic space, ‘A’ – attribute, and ‘W’ – word vector.

Dataset	#instances	SS	SS-D	#seen/unseen
AwA	30,475	A	85	40/10
CUB	11,788	A	312	150/50
SUN	14,340	A	102	645/72
ImNet	218,000	W	1,000	1,000/360

our hierarchy are shared across the two domains, our projection learning method can alleviate the projection domain shift and thus benefit unseen class image recognition. By combining class hierarchy construction, deep feature learning, and projection function learning together for inductive ZSL, our full algorithm is outlined in Algorithm 2.

3.5 Extension to Few-Shot Learning

Although the proposed model is originally designed for ZSL, it can be easily extended to FSL. Under a standard FSL setting, the dataset is split into three parts: a training set of many labelled base/seen class samples, a support set of few labelled novel/unseen class samples, and a test set of the rest novel class samples. In this work, we first construct a tree-structured class hierarchy using all base and novel class prototypes as in Sec. 3.2. With the obtained class hierarchy, we further train our full model (including deep feature learning and projection function learning) over the whole training set as before, and predict the labels of test samples as in Sec. 3.4.2. To obtain better FSL results, we exploit both average visual features of few shot samples per novel class and the projected novel class prototypes for nearest neighbor search in the feature space.

4 Experiments

4.1 Zero-Shot Learning

4.1.1 Datasets and Settings

Datasets. Four widely-used benchmark datasets are selected. Three of them are of medium-size: Animals with Attributes (AwA) (Lampert et al., 2014), Caltech UCSD Birds (CUB) (Wah et al., 2011), and SUN Attribute (SUN) (Patterson et al., 2014). One large-scale dataset is ILSVRC2012/2010 (ImNet)(Russakovsky et al., 2015), where the 1,000 classes of ILSVRC2012 are used as seen classes and 360 classes of ILSVRC2010 (not included in ILSVRC2012) are used as unseen classes, as in (Fu and Sigal, 2016). The details of these benchmark datasets are given in Table 1.

Semantic Space. We use two types of semantic spaces. For the three medium-scale datasets, attributes are used

as the semantic representations. For the large-scale ImNet dataset, the semantic word vectors are employed to form the semantic space. In this paper, we train a skip-gram text model on a corpus of 4.6M Wikipedia documents to obtain the word2vec (Norouzi et al., 2014) word vectors.

ZSL Settings. (1) Standard ZSL: This ZSL setting is used in pre-2017 works (Kodirov et al., 2015, 2017; Zhang and Saligrama, 2015, 2016a; Akata et al., 2015; Zhang and Saligrama, 2016b). Concretely, the train/test (or seen/unseen classes) splits of 40/10, 150/50, 645/72, and 1,000/360 are provided for AwA, CUB, SUN, and ImNet, respectively. (2) Pure ZSL: A new ‘pure’ ZSL setting (Xian et al., 2017) was proposed to overcome the weakness in the standard ZSL setting. Specifically, most recent ZSL models extract the visual features using ImageNet ILSVRC2012 1K class pretrained CNN models, but the unseen classes of the three medium-scale datasets in the standard splits may overlap with the 1K ImageNet classes. The zero-shot rule is thus violated. Under the new ZSL setting, new benchmark splits are provided to ensure that the unseen classes have no overlap with the ImageNet ILSVRC2012 1K classes. (3) Generalised ZSL: Another recently appearing setting is the generalised ZSL setting (Xian et al., 2017), under which the test set contains data samples from both seen and unseen classes. This setting is more suitable for real-world applications.

Evaluation Metrics. (1) Standard ZSL: For three medium-scale datasets, we compute the top-1 classification accuracy over all test samples as in previous works (Kodirov et al., 2015; Zhang and Saligrama, 2015, 2016a). (2) Pure ZSL: For three medium-scale datasets, we compute average per-class top-1 accuracy as in (Xian et al., 2017). For the large-scale ImNet dataset, the flat h@5 classification accuracy is computed as in (Fu and Sigal, 2016; Kodirov et al., 2017), where h@5 means that a test image is classified to a ‘correct label’ if it is among the top five labels. (3) Generalised ZSL: Three evaluation metrics are defined: 1) acc_s – the accuracy of classifying the data samples from the seen classes to all the classes (both seen and unseen); 2) acc_u – the accuracy of classifying the data samples from the unseen classes to all the classes; 3) HM – the harmonic mean of acc_s and acc_u .

Compared Methods. A wide range of existing ZSL models are selected for comparison. Under each ZSL setting, we focus on the recent and representative ZSL models that have achieved the state-of-the-art results.

4.1.2 Implementation Details

Class Hierarchy Construction. $R = \{r_l : l = 1, \dots, n_r\}$ that collects the number of clusters (i.e. r_l) at each superclass layer of the tree-structured class hierarchy (with n_r superclass layers) is empirically defined as: $r_l = \lfloor (p + q)/t^{l-2} \rfloor$. n_r is determined with the constraint that each layer has at least t nodes. To study the influence of t

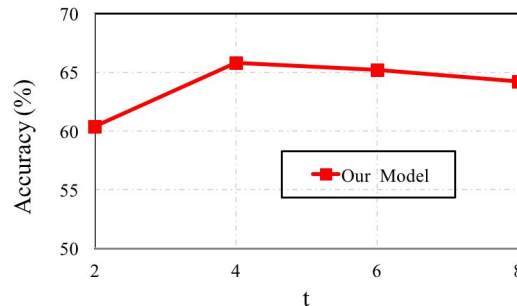


Fig. 3 Illustration of the effect of the parameter t on our model under the pure ZSL setting for the CUB dataset.

on our model, we provide the results of our model with different hierarchy structures (determined by the parameter t) in Fig. 3. We can observe that the performance will drop when t becomes oversize (e.g. $t = 8$). It is reasonable that the oversize parameter t leads to a very shallow hierarchy and the improvements brought by our model thus diminish. Therefore, to better select the parameter t , we perform cross-validation on the training data, as in (Kodirov et al., 2017).

Deep Network Training. In our CNN-RNN model, the first five groups of convolutional layers in VGG-16 Net (Simonyan and Zisserman, 2014) are used as the CNN subnet. The convolutional layers of this CNN subnet are pre-trained on ILSVRC 2012 (Russakovsky et al., 2015), while the other layers (including the LSTMs) are trained from scratch. Stochastic gradient descent (SGD) (LeCun et al., 1989) is used for model training with a base learning rate of 0.001. For those layers trained from scratch, their learning rates are 10 times of the base learning rate. The deep learning is implemented with Caffe (Jia et al., 2014).

Projection Function Learning. Our projection function learning model has three groups of parameters to tune: $\{\alpha^l : l = 1, \dots, n_r\}$ (in Eq. (10)), $\{\beta^l : l = 1, \dots, n_r\}$ (in Eq. (12)), and $\{\epsilon^l : l = 1, \dots, n_r\}$ (in Eq. (12)). In this paper, we select $\alpha^1, \beta^1, \epsilon^1$ by cross-validation on the training data as in (Kodirov et al., 2017). Then, we directly use them in other superclass-level projection learning and class-level projection learning (in Eq. (13)).

4.1.3 Comparative Evaluation

Standard ZSL. Table 2 shows the results of the comparison to the state-of-the-art ZSL models under the standard ZSL setting. We can obtain the following observations: (1) Our full model for inductive ZSL clearly outperforms the state-of-the-art inductive alternatives. Particularly, the improvements obtained by our model over the strongest inductive competitor are significant for AwA, CUB, and SUN, i.e. 3.9%, 5.8%, and 4.4%, respectively. This validates the effectiveness of our model for inductive ZSL. (2) Our model even yields significantly better results than some recent transductive ZSL models. This is really impressive

Table 2 Comparative accuracies (%) of standard ZSL. Visual features: GOO – GoogLeNet (Szegedy et al., 2015); VGG – VGG Net (Simonyan and Zisserman, 2014); RES – ResNet (He et al., 2016); Feat-Learn – deep feature learning.

Model	Visual Features	Inductive?	AwA	CUB	SUN
SP-ZSR (Zhang and Saligrama, 2016b)	VGG	no	92.1	55.3	–
SSZSL (Shojaee and Baghshah, 2016)	VGG	no	88.6	58.8	–
DSRL (Ye and Guo, 2017)	VGG	no	87.2	57.1	–
TSTD (Yu et al., 2017)	VGG	no	90.3	58.2	–
BiDiLEL (Wang and Chen, 2017)	VGG	no	95.0	62.8	–
DMAp (Li et al., 2017b)	VGG+GOO+RES	no	90.5	67.7	–
DLSE (Zhang and Saligrama, 2016a)	VGG	yes	80.5	42.1	–
LAD (Jiang et al., 2017)	VGG	yes	82.5	56.6	–
SCoRe (Morgado and Vasconcelos, 2017)	VGG	yes	82.8	59.5	–
LESD (Ding et al., 2017)	VGG	yes	82.8	56.2	–
SJE (Akata et al., 2015)	GOO	yes	73.9	51.7	56.1
SynC (Changpinyo et al., 2016)	GOO	yes	72.9	54.7	62.7
VZSL (Wang et al., 2018)	VGG	yes	85.3	57.4	–
SAE (Kodirov et al., 2017)	GOO	yes	84.7	61.4	65.2
CVAE (Mishra et al., 2017)	RES	yes	85.8	54.3	–
CLN+KRR (Long et al., 2017)	Feat-Learn	yes	81.0	58.6	–
GVR (Bucher et al., 2017)	Feat-Learn	yes	87.8	60.1	56.4
Ours	Feat-Learn	yes	91.7	67.2	69.6

Table 3 Comparative accuracies (%) of pure ZSL. For ImNet, the hit@5 accuracy is used. The notations are the same as in Table 2.

Model	Visual Features	AwA	CUB	SUN	ImNet
CMT (Socher et al., 2013)	RES	39.5	34.6	39.9	–
DeViSE (Frome et al., 2013)	RES	54.2	52.0	56.5	12.8
DAP (Lampert et al., 2014)	RES	44.1	40.0	39.9	–
ConSE (Norouzi et al., 2014)	RES	45.6	34.3	38.8	15.5
SSE (Zhang and Saligrama, 2015)	RES	60.1	43.9	51.5	–
SJE (Akata et al., 2015)	RES	65.6	53.9	53.7	–
ALE (Zhang and Saligrama, 2016a)	RES	59.9	54.9	58.1	–
SynC (Changpinyo et al., 2016)	RES	54.0	55.6	56.3	–
SP-AEN (Chen et al., 2018)	RES	58.5	55.4	59.2	–
CVAE (Mishra et al., 2017)	VGG	71.4	52.1	61.7	24.7
SAE (Kodirov et al., 2017)	GOO	61.3	48.2	59.2	27.2
DEM (Zhang et al., 2017)	GOO	68.4	51.7	61.9	25.7
CLN+KRR (Long et al., 2017)	Feat-Learn	68.2	58.1	60.0	–
WGAN+ALE (Xian et al., 2018)	Feat-Learn	68.2	61.5	62.0	–
Ours	Feat-Learn	72.2	65.8	62.9	28.6

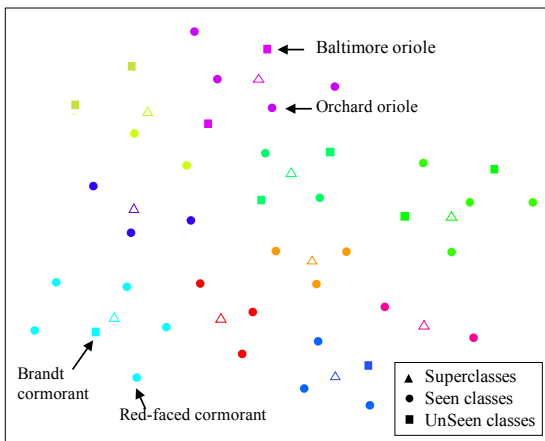
given that these transductive models have access to the full test data for model training and thus have an inherent advantage over the inductive ZSL models including ours. (3) All recent inductive ZSL models that induce deep feature learning into ZSL are quite competitive, as compared to those without deep feature learning. Among these deep feature learning models, our model clearly performs the best thanks to transferrable feature learning with the superclasses from the proposed class hierarchy.

Pure ZSL. By following the same ‘pure’ ZSL setting in (Xian et al., 2017), the overlapped ImageNet ILSVRC2012 1K classes are removed from the test set of unseen classes for the three medium-scale datasets, while the split of the ImNet dataset naturally satisfies the ‘pure’ ZSL setting. Table 3 presents the comparative results under the pure

ZSL setting. It can be seen that: (1) Our model yields the best results on all four datasets and achieves about 1-4% performance improvement over the best competitors. This validates the effectiveness of our model for this stricter ZSL setting. (2) On the large-scale ImNet dataset, our model achieves about 1–4% improvements over the state-of-the-art ZSL models (Mishra et al., 2017; Kodirov et al., 2017; Zhang et al., 2017), showing the scalability of our model for large-scale ZSL problems. (3) Our model clearly outperforms the state-of-the-art feature learning model (Xian et al., 2018), due to our transferrable feature and projection learning with the superclasses. This is also supported by the t-SNE visualisation of the superclasses in Fig. 4, where an unseen class tends to be semantically related to a seen class

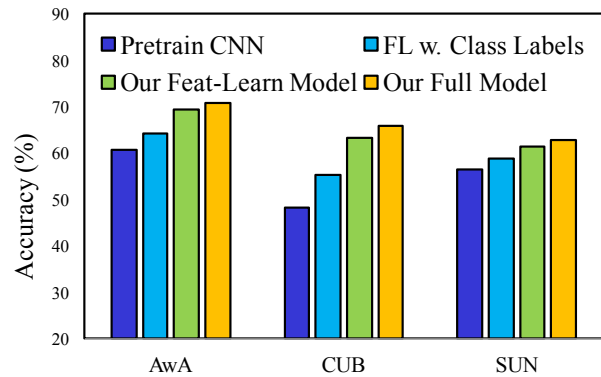
Table 4 Comparative results (%) of generalised ZSL. The *overall* performance is evaluated by the HM metric.

Model	AwA			CUB			SUN		
	acc_s	acc_u	HM	acc_s	acc_u	HM	acc_s	acc_u	HM
CMT (Socher et al., 2013)	86.9	8.4	15.3	60.1	4.7	8.7	28.0	8.7	13.3
DeViSE (Frome et al., 2013)	68.7	13.4	22.4	53.0	23.8	32.8	27.4	16.9	20.9
SSE (Zhang and Saligrama, 2015)	80.5	7.0	12.9	46.9	8.5	14.4	36.4	2.1	4.0
SJE (Akata et al., 2015)	74.6	11.3	19.6	59.2	23.5	33.6	30.5	14.7	19.8
LATEM (Xian et al., 2016)	71.7	7.3	13.3	57.3	15.2	24.0	28.8	14.7	19.5
ALE (Akata et al., 2016)	76.1	16.8	27.5	62.8	23.7	34.4	33.1	21.8	26.3
ESZSL (Romera-Paredes and Torr, 2015)	75.6	6.6	12.1	63.8	12.6	21.0	27.9	11.0	15.8
SynC (Changpinyo et al., 2016)	87.3	8.9	16.2	70.9	11.5	19.8	43.3	7.9	13.4
SAE (Kodirov et al., 2017)	71.3	31.5	43.5	36.1	28.0	31.5	25.0	15.8	19.4
DEM (Zhang et al., 2017)	84.7	32.8	47.3	57.9	19.6	29.2	34.3	20.5	25.6
SP-AEN (Chen et al., 2018)	90.9	23.3	37.1	70.6	34.7	46.6	38.6	24.9	30.3
WGAN+ALE (Xian et al., 2018)	57.2	47.6	52.0	59.3	40.2	47.9	31.1	41.3	35.5
Ours	68.2	44.5	53.9	46.9	51.1	48.9	30.2	31.4	30.7

**Fig. 4** The t-SNE visualisation of the superclasses generated by clustering on the CUB dataset. For easy viewing, we randomly choose 10 superclasses (marked with different colors).

within the same superclass (i.e. the superclasses are shared across the seen and unseen domains).

Generalised ZSL. We follow the same generalised ZSL setting of (Xian et al., 2017). Table 4 provides the comparative results of generalised ZSL on the three medium-scale datasets. We can observe that: (1) Different ZSL models take a different trade-off between acc_u and acc_s , and the overall performance is thus measured by the HM metric. (2) Our model achieves similar results on seen and unseen class domains while existing models favor one over the other. That is, our model has the strongest generalisation ability under this more challenging setting. (3) Our model clearly yields the best overall performance on AwA and CUB datasets, while is outperformed by the state-of-the-art model (Xian et al., 2018) on the SUN dataset. This is still very impressive, given that (Xian et al., 2018) exploits

**Fig. 5** Ablation study results on the three medium-scale datasets under the pure ZSL setting.

a much superior CNN model (i.e. ResNet-101 (He et al., 2016)) for feature extraction.

4.1.4 Further Evaluations

Ablation Study. We compare our full model with a number of striped-down versions to evaluate the effectiveness of the key components of our model. Three of such feature learning models are compared, each of which uses the same projection learning model (i.e. the baseline model defined by Eq. (7), where only class-level semantics are exploited) and differs only in how the visual features are obtained: ‘Pretrain CNN’ – the same CNN model trained on ImageNet without any finetuning on seen class data; ‘FL w. Class Labels’ – feature learning by finetuning with only class labels of seen class images; ‘Our Feat-Learn Model’: feature learning by the proposed model in Sec. 3.3. The ablation study results in Fig. 5 show that: (1) The transferrable feature learning with the class hierarchy leads to significant improvements

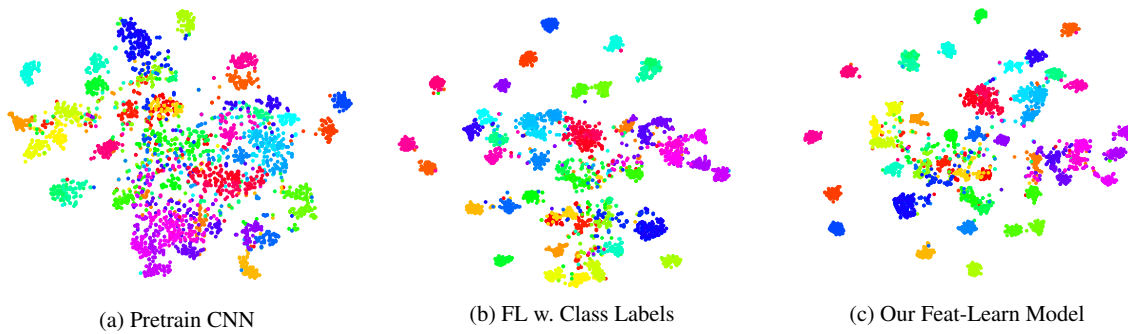


Fig. 6 The tSNE visualisation of the visual features of the test unseen class samples from the CUB dataset. The visual features of test samples are obtained by the feature learning methods used in the ablation study, while the labels (marked with different colors) of test samples are directly set as the ground-truth labels and thus keep fixed.

Unseen class images	Candidate Classes	Unseen class images	Candidate Classes
	Common tern ; California gull; Glaucous winged gull; Herring gull; Ivory gull; Ring billed gull ; Western gull; Red legged kittiwake; Artic tern ; Caspian tern; Laysan albatross; Elegant tern ; Forster's tern; Least tern ;		Red bellied woodpecker ; Least auklet; Pied kingfisher; Black and white warbler; Red cockaded woodpecker ; Crested auklet; Red headed woodpecker; Parakeet auklet; Downy woodpecker ; Horned puffin; Rose breasted grosbeak; Pigeon guillemot ; American three toed woodpecker
	Green kingfisher ; Sooty albatross; Black footed albatross; Eared grebe; Horned grebe; Western grebe ; Long tailed jaeger; Pacific loon; Pomarine jaeger ; Belted kingfisher; Ringed kingfisher ; Brown pelican; Hooded merganser; Black tern ;		Cape May warbler ; Evening grosbeak; Yellow throated vireo; Hooded warbler ; Blue winged warbler ; Kentucky warbler; Magnolia warbler; Mourning warbler; Nashville warbler; Pine warbler ; Prairie warbler; Common yellowthroat
	Least flycatcher ; Mangrove cuckoo; Acadian flycatcher; Mockingbird; Great crested flycatcher; Palm warbler ; Olive sided flycatcher; Warbling vireo; Yellow bellied flycatcher ; Sayornis; Western wood pewee; Seaside sparrow ; Bank swallow; Red eyed vireo;		Tree sparrow ; Gray crowned rosy finch; American Pipit; Whip poor will; Baird sparrow ; Brewer sparrow; Chipping sparrow; Clay colored sparrow; House sparrow; Fieldsparrow; Grasshopper Sparrow; Harris_Sparrow ; Henslow sparrow ; Vesper sparrow;
	Baltimore oriole ; Brewer blackbird; Eastern towhee; American redstart; Shiny cowbird ; Boat tailed grackle; Orchard oriole; White necked raven; Yellow headed blackbird; Bobolink; Hooded oriole; Scott oriole		Winter wren ; Chuck will widow; Fox sparrow; Lincoln sparrow; Savannah sparrow; Song sparrow ; Brown thrasher; Northern waterthrush; Carolina wren; House wren ; Cactus wren; Bewick wren ; Marsh wren; Wilson warbler

Fig. 7 Examples of candidate classes obtained by our ZSL model. The seen class candidates are in blue, unseen class candidates are in red, and the ground truth labels are in red bold. The number of candidate classes for each unseen class sample is forced to become smaller by projection function learning with superclasses.

(see Our Feat-Learn Model vs. FL w. Class Labels), ranging from 3% to 9%. This provides strong supports for our main contribution on deep feature learning for ZSL. (2) Our full model with extra transferrable projection learning achieves about 1–2% improvements (see Our Full Model vs. Our Feat-Learn Model), showing the effectiveness of our transferrable projection learning for inductive ZSL. (3) As expected, finetuning the CNN model can learn better deep features for ZSL, yielding 2–7% gains. However, the finetuned CNN model can not extract transferrable features and thus has very limited practicality.

Qualitative Results. We provide qualitative results to show why adding more components into our feature learning model benefits ZSL in the above ablation study. Fig. 6 shows the tSNE visualisation of the visual features of test unseen class samples. The visual features of test unseen class samples are obtained by the feature learning methods used in the above ablation study, while the labels of test unseen class samples are directly set as the ground-truth labels and thus keep fixed. It can be clearly seen that the visual features of the test samples become more separable when more components are added into our feature learning model, enabling us to obtain better recognition results.

Table 5 Comparative h@5 classification accuracies obtained by using the human-annotated/our hierarchy on the ImNet dataset.

Model	Human-annotated	Ours
Our Feat-Learn Model	27.8	28.0
Our Full Model	28.3	28.6

Table 6 Comparative classification accuracies obtained by using the human-annotated/our hierarchy on the CUB dataset.

Model	Human-annotated	Ours
Our Feat-Learn Model	64.6	64.7
Our Full Model	65.6	65.8

In addition, some qualitative results are given to show how the proposed projection learning method benefits unseen class recognition. Fig. 7 presents examples of candidate classes obtained by projection learning with superclasses. In this figure, the seen class candidates are in blue, unseen class candidates are in red, and the ground truth labels are in bold. According to Algorithm 1, our projection learning method finds the best predicted label for each test image by nearest neighbor searching among unseen classes in several superclasses, rather than search among all unseen classes. This explains the superior performance of our projection learning method using superclasses.

Human-Annotated Class Hierarchy. The proposed ZSL model can be easily generalised to the human-annotated tree-structured class hierarchy (e.g. the biological taxonomy tree for animal classes, and the hierarchy tree of object classes provided by ImageNet). Concretely, we directly use seen/unseen classes as the bottom class layer and the higher-level classes are thus assigned as superclass layers (e.g. for animal classes, genus-level, family-level, and order-level layers can be used as superclass layers). Similarly, we can learn transferrable deep features by using the proposed feature learning model in Sec. 3.3. With the learned features, we can infer the labels of test unseen class images by using the proposed projection learning method in Sec. 3.4.

Tables 5 and 6 give the comparative classification results with the human-annotated class hierarchy and our class hierarchy on the ImNet and CUB datasets under the pure ZSL setting, respectively. The human-annotated class hierarchy used in the CUB dataset is the biological taxonomy tree collected from Wikipedia, while the human-annotated class hierarchy used in the ImNet dataset is collected by WordNet² (Miller, 1995). As shown in these two tables, our class hierarchy has achieved better performance than the human-annotated class hierarchy. This is reasonable because the human-annotated class hierarchy is prone to the superclass imbalance (i.e. the number of classes belonging to different superclasses varies greatly), while our class hierarchy often provides more balanced clustering results.

² The class hierarchy is available at <http://www.image-net.org>.

4.2 Few-Shot Learning

4.2.1 Dataset and Settings

To directly compare our method to the standard few-shot learning methods (Snell and Zemel, 2017; Qiao et al., 2018; Finn et al., 2017; Sung et al., 2018; Triantafillou et al., 2017; Mishra et al., 2017; Vinyals et al., 2016), we further apply it to FSL on mini-ImageNet as in (Snell and Zemel, 2017). This dataset consists of 100 ImageNet classes, which is significantly smaller than the large-scale ImNet. The semantic space is formed as in Sec. 4.1.1, while the visual features are extracted with two CNN models trained from scratch with the training set of mini-ImageNet: (1) Simple - four conventional blocks as in (Snell and Zemel, 2017); (2) WRN - wide residual networks (Zagoruyko and Komodakis, 2016) as in (Qiao et al., 2018). The 5-way accuracy is computed by randomly selecting 5 classes from the 20 novel classes for each test trial, and the average accuracy over 600 test trials is used as the evaluation metric.

4.2.2 Comparative Evaluation

The comparative 5-way accuracies on mini-ImageNet are given in Table 7. We can make the following observations: (1) Our model achieves state-of-the-art performance under the 5-way 5-shot setting and competitive results under 5-way 1-shot. This suggests that our model is effective not only for ZSL but also for FSL. (2) Stronger visual features extracted for FSL yield significantly better results, when PPA and our model are concerned.

5 Conclusion

In this paper, we tackle the domain gap challenge in ZSL by leveraging superclasses as the bridge between seen and unseen classes. We first build a tree-structured class hierarchy that consists several superclass layers and one single class layer. Then, we exploit the superclasses to overcome the domain gap challenge in two aspects: deep feature learning and projection function learning. In the deep feature learning phase, we introduce a recurrent neural network (RNN) defined with the superclasses from the class hierarchy into a convolutional neural network (CNN). A novel CNN-RNN model is thus proposed for transferrable deep feature learning. In the projection function learning phrase, we align the seen and unsee class domains using the superclasses from the class hierarchy. Extensive experiments on four benchmark datasets show that the proposed ZSL model yields significantly better results than the state-of-the-art alternatives. Furthermore, our model can be extended to few-shot learning and also achieves promising results. In our

Table 7 Comparative 5-way accuracies (%) with 95% confidence intervals for FSL on mini-ImageNet.

Model	CNN	1 shot	5 shot
Nearest Neighbor	Simple	41.8±0.70	51.04±0.65
Matching Net (Vinyals et al., 2016)	Simple	43.56±0.84	55.31±0.73
Meta-Learn LSTM(Ravi and Larochelle, 2016)	Simple	43.33±0.77	60.60±0.71
MAML(Finn et al., 2017)	Simple	48.70±1.84	63.11±0.92
Prototypical Net (Snell and Zemel, 2017)	Simple	49.42±0.78	68.20±0.66
mAP-SSVM(Triantafillou et al., 2017)	Simple	50.32±0.80	63.94±0.72
Relation Net(Sung et al., 2018)	Simple	50.44±0.82	65.32±0.70
SNAIL(Mishra et al., 2016)	ResNet20	55.71±0.99	68.88±0.92
PPA(Qiao et al., 2018)	Simple	54.53±0.40	67.87±0.20
PPA(Qiao et al., 2018)	WRN	59.60±0.41	73.74±0.19
Ours	Simple	53.92±0.63	65.13±0.61
Ours	WRN	57.14±0.78	74.45±0.73

ongoing research, we would implement our current projection learning method using a deep autoencoder framework and then connect it to the CNN-RNN model so that the entire network can be trained in an end-to-end manner. Moreover, we also expect that our CNN-RNN model can be generalised to other ZSL-related vision problems such as multi-label ZSL and large-scale FSL.

Acknowledgements This work was supported in part by National Natural Science Foundation of China (61573363 and 61573026), Beijing Natural Science Foundation (L172037), 973 Program of China (2015CB352502), the Fundamental Research Funds for the Central Universities and the Research Funds of Renmin University of China (15XNLQ01), and European Research Council FP7 Project SUNNY (313243).

References

- Akata Z, Reed S, Walter D, Lee H, Schiele B (2015) Evaluation of output embeddings for fine-grained image classification. In: Proc. CVPR, pp 2927–2936
- Akata Z, Perronnin F, Harchaoui Z, Schmid C (2016) Label-embedding for image classification. *IEEE Trans Pattern Analysis and Machine Intelligence* 38(7):1425–1438
- Alexiou I, Xiang T, Gong S (2016) Exploring synonyms as context in zero-shot action recognition. In: Proc. IEEE Conference on Image Processing, pp 4190–4194
- Bartels RH, Stewart GW (1972) Solution of the matrix equation $ax + xb = c$ [f4]. *Communications of the ACM* 15:820–826
- Bucher M, Herbin S, Jurie F (2017) Generating visual representations for zero-shot classification. In: ICCV Workshops: Transferring and Adapting Source Knowledge in Computer Vision, pp 2666–2673
- Changpinyo S, Chao WL, Gong B, Sha F (2016) Synthesized classifiers for zero-shot learning. In: Proc. CVPR, pp 5327–5336
- Chao WL, Changpinyo S, Gong B, Sha F (2016) An empirical study and analysis of generalized zero-shot learning for object recognition in the wild. In: Proc. ECCV, pp 52–68
- Chen L, Zhang H, Xiao J, Liu W, Chang SF (2018) Zero-shot visual recognition using semantics-preserving adversarial embedding network. In: Proc. CVPR
- Deng J, Ding N, Jia Y, Frome A, Murphy K, Bengio S, Li Y, Neven H, Adam H (2014) Large-scale object classification using label relation graphs. In: Proc. ECCV, pp 48–64
- Ding Z, Shao M, Fu Y (2017) Low-rank embedded ensemble semantic dictionary for zero-shot learning. In: Proc. CVPR, pp 2050–2057
- Donahue J, Jia Y, Vinyals O, Hoffman J, Zhang N, Tzeng E, Darrell T (2014) DeCAF: A deep convolutional activation feature for generic visual recognition. In: Proc. ICML, pp 647–655
- Finn C, Abbeel P, Levine S (2017) Model-agnostic meta-learning for fast adaptation of deep networks. In: Proc. ICML, pp 1126–1135
- Frome A, Corrado GS, Shlens J, Bengio S, Dean J, Ranzato MA, Mikolov T (2013) DeViSE: A deep visual-semantic embedding model. In: NIPS, pp 2121–2129
- Fu Y, Sigal L (2016) Semi-supervised vocabulary-informed learning. In: Proc. CVPR, pp 5337–5346
- Fu Y, Hospedales TM, Xiang T, Gong S (2015a) Transductive multi-view zero-shot learning. *IEEE Trans Pattern Analysis and Machine Intelligence* 37(11):2332–2345
- Fu Z, Xiang T, Kodirov E, Gong S (2015b) Zero-shot object recognition by semantic manifold distance. In: Proc. CVPR, pp 2635–2644
- Graves A, Mohamed Ar, Hinton GE (2013) Speech recognition with deep recurrent neural networks. In: Proc. ICASSP, pp 6645–6649
- Guo Y, Ding G, Jin X, Wang J (2016) Transductive zero-shot recognition via shared model space learning. In: Proc. AAAI Conference on Artificial Intelligence, pp 3494–3500

- He K, Zhang X, Ren S, Sun J (2016) Deep residual learning for image recognition. In: Proc. CVPR, pp 770–778
- Huang G, Liu Z, Maaten Lvd, Weinberger KQ (2017) Densely connected convolutional networks. In: Proc. CVPR, pp 2261–2269
- Hwang SJ, Sigal L (2014) A unified semantic embedding: Relating taxonomies and attributes. In: NIPS, pp 271–279
- Jia Y, Shelhamer E, Donahue J, Karayev S, Long J, Girshick R, Guadarrama S, Darrell T (2014) Caffe: Convolutional architecture for fast feature embedding. arXiv preprint arXiv:14085093
- Jiang H, Wang R, Shan S, Yang Y, Chen X (2017) Learning discriminative latent attributes for zero-shot classification. In: Proc. ICCV, pp 4223–4232
- Kodirov E, Xiang T, Fu Z, Gong S (2015) Unsupervised domain adaptation for zero-shot learning. In: Proc. ICCV, pp 2452–2460
- Kodirov E, Xiang T, Gong S (2017) Semantic autoencoder for zero-shot learning. In: Proc. CVPR, pp 3174–3183
- Lampert CH, Nickisch H, Harmeling S (2014) Attribute-based classification for zero-shot visual object categorization. *IEEE Trans Pattern Analysis and Machine Intelligence* 36(3):453–465
- LeCun Y, Boser BE, Denker JS, Henderson D, Howard RE, Hubbard LD, Wayne E and Jackel (1989) Backpropagation applied to handwritten zip code recognition. *Neural Computation* 1(4):541–551
- Li A, Lu Z, Wang L, Xiang T, Wen JR (2017a) Zero-shot scene classification for high spatial resolution remote sensing images. *IEEE Trans Geoscience and Remote Sens* 55(7):4157–4167
- Li X, Guo Y, Schuurmans D (2015) Semi-supervised zero-shot classification with label representation learning. In: Proc. ICCV, pp 4211–4219
- Li Y, Wang D, Hu H, Lin Y, Zhuang Y (2017b) Zero-shot recognition using dual visual-semantic mapping paths. In: Proc. CVPR, pp 5207–5215
- Liu F, Xiang T, Hospedales TM, Yang W, Sun C (2017) Semantic regularisation for recurrent image annotation. In: Proc. CVPR, pp 4160–4168
- Long T, Xu X, Shen F, Liu L, Xie N, Yang Y (2017) Zero-shot learning via discriminative representation extraction. *Pattern Recognition Letters* DOI: 10.1016/j.patrec.2017.09.030
- Miller GA (1995) Wordnet: An online lexical database. *Communications of the ACM* 38(11):39–44
- Mishra A, Reddy MSK, Mittal A, Murthy HA (2017) A generative model for zero shot learning using conditional variational autoencoders. In: arXiv preprint arXiv:1709.00663
- Mishra N, Rohaninejad M, Chen X, Abbeel P (2016) A simple neural attentive meta-learner. In: Proc. ICLR
- Morgado P, Vasconcelos N (2017) Semantically consistent regularization for zero-shot recognition. In: Proc. CVPR, pp 6060–6069
- Norouzi M, Mikolov T, Bengio S, Singer Y, Shlens J, Frome A, Corrado GS, Dean J (2014) Zero-shot learning by convex combination of semantic embeddings. In: Proc. ICLR
- Patterson G, Xu C, Su H, Hays J (2014) The sun attribute database: Beyond categories for deeper scene understanding. *International Journal of Computer Vision* 108(1):59–81
- Qiao S, Liu C, Shen W, , Yuille AL (2018) Few-shot image recognition by predicting parameters from activations. In: Proc. CVPR, pp 7229–7238
- Rahman S, Khan SH, Porikli F (2017) A unified approach for conventional zero-shot, generalized zero-shot and few-shot learning. arXiv preprint arXiv:170608653
- Ravi S, Larochelle H (2016) Optimization as a model for few-shot learning. In: Proc. ICLR
- Reed S, Akata Z, Lee H, Schiele B (2016) Learning deep representations of fine-grained visual descriptions. In: Proc. CVPR, pp 49–58
- Rohrbach M, Ebert S, Schiele B (2013) Transfer learning in a transductive setting. In: NIPS, pp 46–54
- Romera-Paredes B, Torr PHS (2015) An embarrassingly simple approach to zero-shot learning. In: Proc. ICML, pp 2152–2161
- Russakovsky O, Deng J, Su H, Krause J, Satheesh S, Ma S, Huang Z, Karpathy A, Khosla A, Bernstein M, Berg AC, Fei-Fei L (2015) ImageNet large scale visual recognition challenge. *International Journal of Computer Vision* 115(3):211–252
- Shojaee SM, Baghshah MS (2016) Semi-supervised zero-shot learning by a clustering-based approach. arXiv preprint arXiv:160509016
- Simonyan K, Zisserman A (2014) Very deep convolutional networks for large-scale image recognition. arXiv preprint arXiv:14091556
- Snell SK, Jake, Zemel RS (2017) Prototypical networks for few-shot learning. In: NIPS, pp 4080–4090
- Socher R, Ganjoo M, Manning CD, Ng A (2013) Zero-shot learning through cross-modal transfer. In: NIPS, pp 935–943
- Sung F, Yang Y, Zhang L, Xiang T, Torr PH, Hospedales TM (2018) Learning to compare: Relation network for few-shot learning. In: Proc. CVPR, pp 1199–1208
- Szegedy C, Liu W, Jia Y, Sermanet P, Reed S, Anguelov D, Erhan D, Vanhoucke V, Rabinovich A (2015) Going deeper with convolutions. In: Proc. CVPR, pp 1–9
- Triantafyllou E, Zemel R, Urtasun R (2017) Few-shot learning through an information retrieval lens. In: NIPS, pp 2255–2265.

- Vinyals O, Blundell C, Lillicrap D, Wainwright J (2016) Matching networks for one shot learning. In: NIPS, pp 3630–3638
- Wah C, Branson S, Welinder P, Perona P, Belongie S (2011) The caltech-ucsd birds-200-2011 dataset. Tech. Rep. CNS-TR-2011-001, California Institute of Technology
- Wang F, Zhang C (2008) Label propagation through linear neighborhoods. *IEEE Trans Knowledge and Data Engineer* 20(1):55–67
- Wang Q, Chen K (2017) Zero-shot visual recognition via bidirectional latent embedding. *International Journal of Computer Vision* 124(3):356–383
- Wang W, Pu Y, Verma VK, Fan K, Zhang Y, Chen C, Rai P, Carin L (2018) Zero-shot learning via class-conditioned deep generative models. In: Proc. AAAI Conference on Artificial Intelligence
- Xian Y, Akata Z, Sharma G, Nguyen Q, Hein M, Schiele B (2016) Latent embeddings for zero-shot classification. In: Proc. CVPR, pp 69–77
- Xian Y, Schiele B, Akata Z (2017) Zero-shot learning - the good, the bad and the ugly. In: Proc. CVPR, pp 4582–4591
- Xian Y, Lorenz T, Schiele B, Akata Z (2018) Feature generating networks for zero-shot learning. In: Proc. CVPR
- Xu X, Hospedales T, Gong S (2015) Semantic embedding space for zero-shot action recognition. In: Proc. IEEE Conference on Image Processing, pp 63–67
- Xu X, Hospedales T, Gong S (2017) Transductive zero-shot action recognition by word-vector embedding. *International Journal of Computer Vision* 123(3):309–333
- Ye M, Guo Y (2017) Zero-shot classification with discriminative semantic representation learning. In: Proc. CVPR, pp 7140–7148
- Yu Y, Ji Z, Li X, Guo J, Zhang Z, Ling H, Wu F (2017) Transductive zero-shot learning with a self-training dictionary approach. arXiv preprint arXiv:170308893
- Zagoruyko S, Komodakis N (2016) Wide residual networks. In: Proc. British Machine Vision Conference, pp 87.1–87.12
- Zhang L, Xiang T, Gong S (2017) Learning a deep embedding model for zero-shot learning. In: Proc. CVPR, pp 2021–2030
- Zhang Z, Saligrama V (2015) Zero-shot learning via semantic similarity embedding. In: Proc. ICCV, pp 4166–4174
- Zhang Z, Saligrama V (2016a) Zero-shot learning via joint latent similarity embedding. In: Proc. CVPR, pp 6034–6042
- Zhang Z, Saligrama V (2016b) Zero-shot recognition via structured prediction. In: Proc. ECCV, pp 533–548
- Zheng S, Jayasumana S, Romera-Paredes B, Vineet V, Su Z, Du D, Huang C, Torr PH (2015) Conditional random fields as recurrent neural networks. In: Proc. CVPR, pp 1529–1537